Vibration Behaviour of Cold-Formed Steel and particleboard Composite Flooring Systems

Suleiman A. AL Hunaity*[1], Harry Far[1a], Ali Saleh[1b]

[1] *School of Civil and Environmental Engineering, Faculty of Engineering and Information Technology, University of Technology Sydney (UTS), Sydney, Australia*

(Received ,Revised ,Accepted)

Abstract: Recently, there has been an increasing demand for buildings that allow rapid assembly of construction elements, have ample open space areas and are flexible in their final intended use. Accordingly, researchers have developed new competitive structures in terms of cost and efficiency, such as cold-formed steel and timber composite floors, to satisfy these requirements. Cold-formed steel and timber composite floors are light floors with relatively high stiffness, which allow for longer spans. As a result, they inherently have lower fundamental natural frequency and lower damping. Therefore, they are likely to undergo unwanted vibrations under the action of human activities such as walking. It is also quite expensive and complex to implement vibration control measures on problematic floors. In this study, a finite element model of a composite floor reported in the literature was developed and validated against four-point bending test results. The validated FE model was then utilised to examine the vibration behaviour of the investigated composite floor. Predictions obtained from the numerical model were compared against predictions from analytical formulas reported in the literature. Finally, the influence of various parameters on the vibration behaviour of the composite floor was studied and discussed.

Keywords: Cold-formed steel, Composite flooring systems, Floor vibrations, Modal analysis, Natural frequency, Finite Element Method

1. Introduction

Open plan floors support sustainable development since they accommodate various use throughout their operational life. As a result, floor structures having large spans with minimum intermediate supports became increasingly of interest in recent years (Ebrahimpour and Sack 1992; Karki and Far 2021). Advances in materials and construction techniques enabled designers to produce slender, light, and long-span floor structures with low stiffness and high ultimate strength, e.g., composite flooring systems or prestressed flat concrete floors (Feldmann *et al.* 2009; Mulas *et al.* 2018). Consequently, these floors may generate resonant or near-resonant structural vibrations, affecting occupants' comfort (Cao *et al.* 2020).

Nowadays, reduction of CO2 emissions and the ever growing population drives the housing sector to implement sustainable and rapid housing schemes (Navaratnam *et al.* 2021). As a result, engineers and stakeholders seek innovative, sustainable, and cost-effective construction methods, such as modular construction, which replaces 70-95% of in situ works activities with off-site modular construction at a designated facility (Thirunavukkarasu *et al.* 2021). Structures manufactured with modular construction are eco-friendly and poses numerous advantages, including higher quality control, cost efficiency, and minimised construction time. Recently, cold-formed steel and timber composite floors have been introduced as an efficient, economical, and durable alternative to traditional concrete floors (Zhang *et al.* 2017). Compared to other traditional construction materials, cold-formed steel provides design flexibility, rapid onsite assembly, dimensional stability, and a high-strength-to-mass ratio (Xu 2011; Loss *et al.* 2016). Recent studies (e.g. Far et al . 2017; Saleh et al. 2018) have also highlighted the benefits of using cold-formed steel members in the

* Corresponding author: PhD candidate, Email: Suleiman.AlHunaity@uts.edu.au
[a] Ph.D., Email: Harry.Far@uts.edu.au
[b] Ph.D., Email: Ali.Saleh@uts.edu.au

building industry. Also, cold-formed steel members are lighter than their hot-rolled counterparts; therefore, the adoption of cold-formed steel members produces lighter structures, ultimately reducing the overall cost and construction time (Gerilla *et al.* 2007; Hsu *et al.* 2014). Moreover, engineered wood products are a sustainable construction material due to their less embodied carbon and energy than concrete. Besides, cold-formed steel and engineered wood products are recyclable materials; thus, they significantly reduce the buildings negative end-of-life impact and promotes a circular economy (Dodoo *et al.* 2014; Navaratnam *et al.* 2021). These advantages show that combining engineered wood products with cold-formed steel sections produces sustainable and cost-effective floors.

However, cold-formed steel and timber flooring systems with lighter weight and longer spans can undergo uncomfortable vibrations caused by human movements. Furthermore, It is quite expensive and challenging to implement vibration control measures in residential and low-rise buildings (Chiniforush *et al.* 2019), emphasising the importance of addressing vibration serviceability at the design stage. A typical cold-formed steel and timber composite floor under construction is shown in Fig. 1. Based on the vibration serviceability, structural floors are generally classified as low-frequency or high-frequency floors (Wyatt 1989; International Organization for Standardization 2007). Low-frequency floors show resonant response when their fundamental natural frequency matches one of the dominant harmonics of a human footstep, and the resonance is maintained by successive footsteps (Bachmann *et al.* 1995; Liu *et al.* 2019). High-frequency floors, on the contrary, experience a transient character vibration response that decays to a relatively insignificant value due to damping before the next footfall is applied (Racic *et al.* 2009). Generally, the fourth harmonic of the walking step frequency is chosen as the cut-off frequency (approximately 10 Hz) to distinguish low and high-frequency floors (Middleton and Brownjohn 2010).

Fig. 1: Typical cold-formed steel and timber composite floor under construction.

Comprehensive studies have been conducted to explore the static performance of cold-formed steel and timber composite floors in terms of the ultimate bearing capacity and the attained degree of composite action, e.g. (Zhu *et al.* 2016; Kyvelou *et al.* 2017, 2018; Zhou *et al.* 2018; Far 2020). Overall, these studies concluded that the stiffness and load-bearing capacity of those floors could be improved provided that adequate composite action is achieved between the cold-formed steel joists and timber panels. Several investigations have been conducted to quantify and assess the vibration performance of cold-formed steel and timber composite flooring systems. Krause (1997) investigated the dynamic behaviour of twenty-five cold-formed steel lightweight composite floors. The study concluded that the Canadian timber floor vibration criteria best assess vibrations in floors supported by cold-formed steel joists. Researchers at the University of Waterloo examined cold-formed steel and timber composite floors (Tangorra *et al.* 2002; Xu and Tangorra 2007; Parnell *et al.* 2010). Laboratory and onsite tests were carried out to evaluate the natural frequency, and mode shapes of the studied floors and identify the key parameters that affect the floor vibrations. The research project concluded that laboratory tested floors represent the worst-case scenario. Similar studies were carried out by

Rack and Lange (2010) and Guan *et al.* (2019). Zhang and Xu (2020) recently proposed a new analytical approach to predict the dynamic behaviour of cold-formed steel and timber composite floors considering three different loading regimes. Based on the new approach, they investigated the effect of different parameters on the dynamic response, including boundary conditions and mass ratios. It was shown that floor response might not be reduced with changing the boundary conditions and that small mass ratios have an insignificant effect on the floor response. Cao *et al.* (2021) conducted in situ testing to evaluate the vibration behaviour of steel composite floors. The study argued that human-structure interaction reduces the damping ratio of the floor. Overall, previous research studies are based on limited structural geometries. The derived acceptance criteria are affected by country norms where the research was conducted; therefore, extending the results into other structural geometries and other countries should be carefully verified (Casagrande *et al.* 2018).

Early studies have suggested limiting the floor static deflection at mid-span to control floor vibrations, pointing out that increasing the floor stiffness will increase its fundamental frequency and minimise vibration response (Mohammed *et al.* 2018). For instance, in Australia, the mid-span deflection limit is 2 mm (Standards Australia 1993). However, a static deflection limit was developed based on the data acquired from residential floors supported by timber joists. Extending such oversimplified design criterion to composite floors supported by cold-formed steel joists may still result in inadequate vibration serviceability.

Even though extensive test results have enhanced the understanding of the vibration response of cold-formed steel lightweight floors, there is still a need for adequate design guidelines and reliable models pertinent to the vibration serviceability of cold-formed steel and timber composite flooring systems (Zhang *et al.* 2017). Thus, further investigations are required to develop the existing pool of data and improve the understanding of the dynamic behaviour of such floors.

The static behaviour of lightweight floors comprised of cold-formed steel joists and particleboards was investigated experimentally and numerically by Kyvelou *et al.* (2017, 2018); however, their vibration serviceability was not considered. However, to the authors' knowledge, no previous numerical or experimental studies exist that evaluate the vibration behaviour of such floors. Therefore, this study aims to numerically investigate the dynamic response of a composite flooring system comprised of cold-formed steel joists and particleboard panels. Using finite element analysis (FEA), it explores the influence of various design parameters on the vibration properties such as natural frequency and non-symmetric mode shapes, which affect how the composite floor performs when excited by human activities at service conditions. In this study, a FE model was created and validated against the results of a four-point bending experimental test under static loading. The validated finite element model is then utilised to investigate the vibration behaviour of the cold-formed steel and timber composite flooring system. Finally, the numerical model is extended to explore the effects of variations in floorboards, joists geometry, and shear connection spacing on the cold-formed steel and timber composite floors' vibration behaviour.

It is highlighted that the vibration performance of a structure could be experimentally evaluated. However, the time and high cost associated with full-scale physical tests, the complexity of raw test data and their post-analysis, and the availability of various types of lightweight floor systems and shear connections render it challenging to investigate the dynamic behaviour of the lightweight floors experimentally (Rainer and Pernica 1986; Pernica 1990; Ebrahimpour and Sack 1992). Thus, it is necessary to develop reliable numerical models that can accurately predict lightweight floors' vibration behaviour, such as cold-formed steel and timber composite flooring systems.

2. Development of the finite element model

Various studies (Loss *et al.* 2016; Zhou *et al.* 2018; Chiniforush *et al.* 2019) have utilised commercial finite element software, such as ANSYS, ABAQUS, and SAP2000, to simulate the behaviour of composite floors subjected to different loading. Chiniforush *et al.* (2019) developed a finite element model of steel-timber composite floors to extend experimental modal testing results by exploring the effects of changing various parameters on the vibration performance of the steel and timber composite floors. Zhou *et al.* (2018) developed a numerical model in ANSYS that accurately captures the non-linear static behaviour of composite floors

fabricated from cold-formed steel and oriented strand timber boards. Loss *et al.* (2016) successfully created a numerical model that precisely simulates experimental push out tests.

This study uses Ansys Workbench (Ansys 2020) to develop and validate the numerical model for the studied cold-formed steel and timber composite floors. The floor is comprised of C-shaped cold-formed steel joists and particle board timber panels. The developed finite element model will be validated against experimental data from four-point bending tests. The model will be then utilised to investigate the vibration behaviour of the composite flooring system. Geometry, material properties, the behaviour of shear connections, and boundary conditions for the investigated composite floor are based on the experimental research work presented by Kyvelou *et al.* (2015, 2017). Details of the developed numerical model and its validation are described in the following sections.

2.1 Geometry of Tested Floors

The investigated floor is comprised of two cold-formed steel joists and two particleboard panels. Each particleboard is 3 m long and 1.2 m wide and has a thickness of 38 mm. Accordingly, cold-formed steel joists are 250 mm deep and have 3.02 mm thickness. The composite floors' total length is 6.0 m; however, the corresponding supported length is 5.8 m. Fig. 2 provides the geometry and dimensions of the tested composite floors. Shear connectors are self-drilling screws and are spaced at 600 mm intervals.

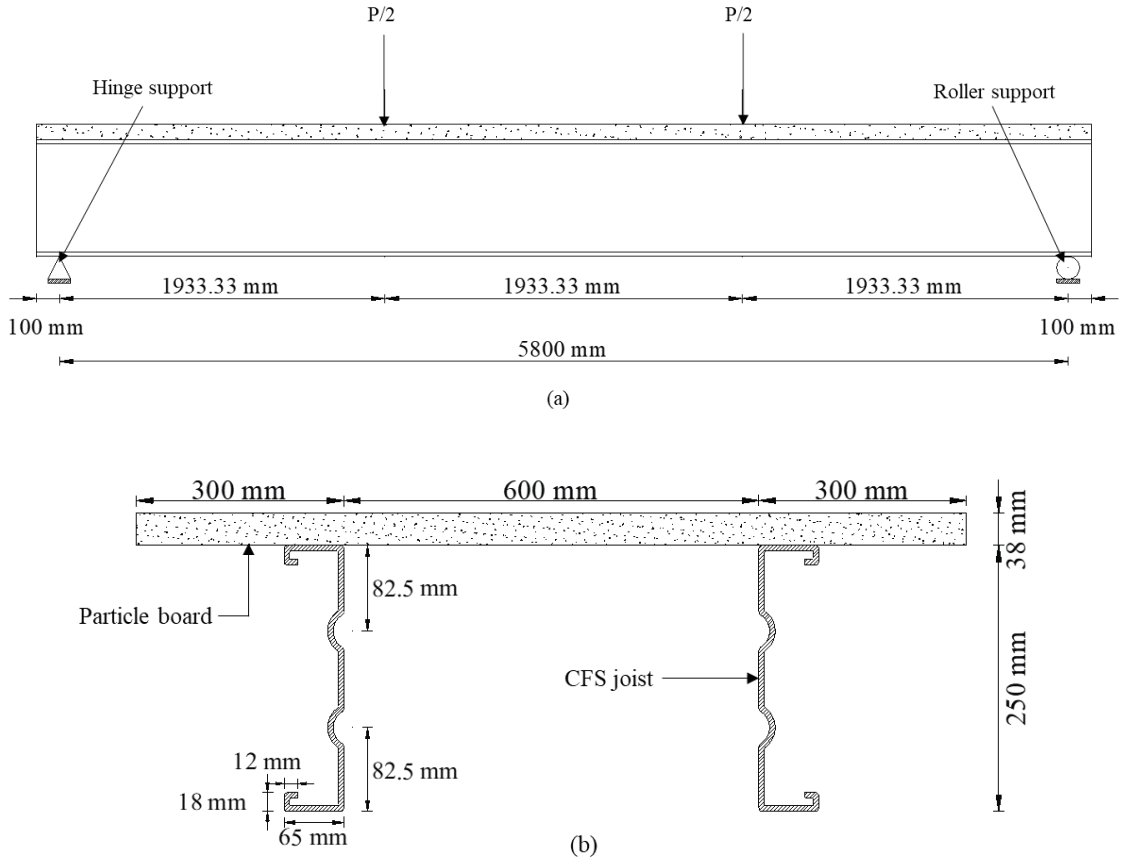

Fig. 2: Geometry and dimensions of tested composite floors (a) Longitudinal, (b) Cross-section.

2.2 Materials Properties

The material properties adopted to validate the developed numerical model is based on the experimental study carried out by Kyvelou *et al.* (2017). The cold-formed steel joists' non-linear behaviour is represented by the two-stage Ramberg-Osgood model (Ramberg and Osgood 1943). Based on this model, Gardner and Ashraf (2006) suggested Eqs. (1)-(2) to describe the non-linear behaviour of metallic materials such as cold-formed steel. Thus, they are utilised to model the non-linear behaviour of the cold-formed steel joists.

$$\varepsilon = \frac{\sigma}{E} + 0.002\left(\frac{\sigma}{\sigma_{0.2}}\right)^{n} \qquad \text{for } \sigma \leq \sigma_{0.2} \tag{1}$$

$$\varepsilon = \varepsilon_{0.2} + \frac{\sigma - \sigma_{0.2}}{E_{0.2}} + \left(\varepsilon_{1.0} - \varepsilon_{0.2} - \frac{\sigma_{1.0} - \sigma_{0.2}}{E_{0.2}}\right)\left(\frac{\sigma - \sigma_{0.2}}{\sigma_{1.0} - \sigma_{0.2}}\right)^{n_{0.2,1}} \quad \text{for } \sigma_{0.2} < \sigma \leq \sigma_{u} \tag{2}$$

where,

σ	is the engineering stress,
ε	is the engineering strain,
E	is Young's modulus of the material,
$\sigma_{0.2}, \sigma_{1.0}$	are the 0.2% and 1.0% proof stresses respectively,
$\varepsilon_{0.2}, \varepsilon_{1.0}$	are the total strains corresponding to 0.2% and 1.0% proof stresses,
$E_{0.2}$	is the tangent modulus of the stress-strain curve at $\sigma_{0.2}$, and
$n, n_{0.2,1.0}$	are the strain hardening components determining the roundedness of stress-strain curve

A summary of the strength properties of the cold-formed steel joists is provided in Table 1. It should be highlighted that although several studies observed higher yield stresses in cold-formed steel sections at corner regions due to accumulations of permanent plastic deformations (Karren 1967; Afshan *et al.* 2013; Kyvelou *et al.* 2017), corner regions and flat regions were assigned the same yield stress value to reduce the model complexity and, hence, the computation time. Finally, stress-strain values obtained from Eqs. (1)-(2) were converted to true stresses and true plastic strains for the input into Ansys software.

Table 1: Mechanical characteristics of the cold-formed steel joists (Kyvelou *et al.* 2018).

Mechanical property	Value
Young's Modulus, E (MPa)	201,000
Poisson's ratio, v	0.3
Flat yield strength, $\sigma_{0.2}$ (MPa)	491
Corner yield strength, $\sigma_{0.2}$ (MPa)	574
Tensile strength, σ_u (MPa)	561
Exponent, n	11.2
Exponent, $n_{0.2,1.0}$	2.1

Behaviour of the particleboards material was determined using Eq. (1) since the stress-strain relationship determined from Eq. (1) correlates well with the experimental results (Kyvelou *et al.* 2017). The values of E and $\sigma_{0.2}$ in Eq. (1) are assumed equal to Young's modulus in compression and compressive strength of the board, respectively. Besides, the value of the exponent n is equal to 6 (Kyvelou *et al.* 2018). Table 2 provides the mechanical characteristics of the particleboard.

Table 2: Mechanical characteristics of the particleboards (Kyvelou *et al.* 2018).

Mechanical property	Value
Young's Modulus, E_b (MPa)	2300
Poisson's ratio ν_b	0.2
Compressive strength, σ_{cb} (MPa)	12.9
Tensile strength, σ_{tb} (MPa)	5.8
Exponent n	6.0

2.3 Element Type and Meshing

Cold-formed steel joists were modelled using standard 4-noded shell elements (SHELL181) with reduced integration formulation. Shell elements can precisely capture local instabilities in structural members with one dimension (thickness) considerably less than the other two dimensions. Additionally, various researchers have adopted shell elements to model steel or cold-formed steel joists, e.g. (Natário *et al.* 2014; Hassanieh *et al.* 2019). On the other hand, 8-noded solid elements (SOLID185) with reduced integration formulation is adopted to model particleboards. Accordingly, several researchers have utilised solid elements to model timber boards or concrete slabs where they could replicate experimental results accurately (Vasdravellis *et al.* 2015; Ataei *et al.* 2016).

The two criteria for selecting the mesh size were capturing the local instabilities in cold-formed steel joists and minimising computational time. Accordingly, ninety-eight shell elements and 186 solid elements were used to model the cross-section of cold-formed steel joists and particle boards, respectively. Besides, corner regions of the cold-formed steel joists are more finely discretised to minimise geometrical errors. The longitudinal mesh size for cold-formed steel joists was taken as 10 mm, and it is set equal to 20 mm for the particleboards. To accurately validate the developed numerical model, the selected mesh density described by Kyvelou et al. (2018) was implemented in this study, which will enable the authors to estimate the vibration behaviour of the cold-formed steel composite floors with sufficient accuracy.

2.4 Modelling of Contacts and Boundary Conditions

A frictional contact was modelled between the lower surface of the particleboards and the top flange of the cold-formed steel joists. The geometric modification – interface treatment option was set to "Adjust to Touch" to prevent excessive penetrations between the particleboards and cold-formed steel joists during the solution. Similarly, frictional contact was assumed at the interface between the two adjacent particle boards. Whereas the friction coefficient between the two adjacent particleboards was taken 0.3, the friction coefficient between particle boards and cold-formed steel joists was set equal to 0.2 (Kyvelou *et al.* 2018).

Fig. 4 provides the details for the imposed boundary conditions. Both ends of each cold-formed steel joist were restrained against vertical and out of plane displacements. An additional constraint in the longitudinal direction was imposed at one end to prevent rigid body motion of the floor during the solution process. Besides, four confining nodes (Fig. 4) were restrained against out-of-plane displacement at points of support and applied forces. Those confining nodes were added to replicate the lateral supports adopted in the physical tests to prevent local failures in the joists. A summary of the adopted boundary conditions is provided in Table 3. It is worth noting that symmetry conditions, applied at the side face of the timber panel along the z-direction,

were considered in the FE model developed by Kyvelou *et al.* (2018). In contrast, this study considers the whole section of the tested floors (Fig. 2b) because the actual geometry of the tested floors is required in the subsequent Modal Analysis to precisely determine its dynamic properties, which include non-symmetric mode shapes.

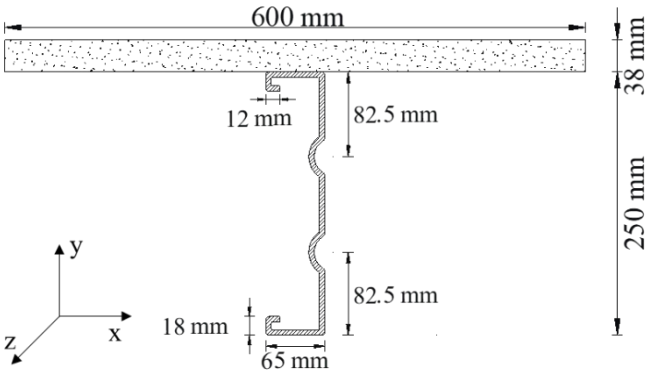

Fig. 3: Adopted cross-section geometry in the FE model developed by Kyvelou *et al.* (2018)

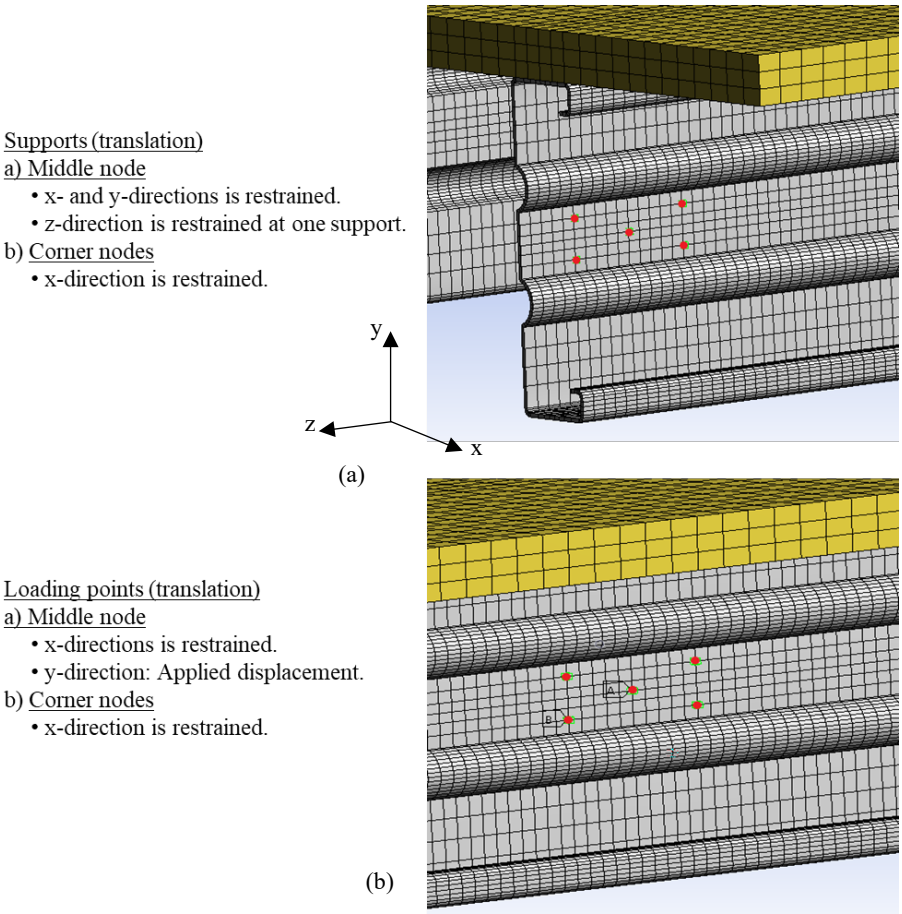

Fig. 4: Adopted arrangement of boundary conditions in the developed FE model at (a) Supports, (b) Loading points.

Table 3: Summary of applied boundary conditions

Location	Boundary Condition
Front support	Translation in x, y, and z directions is restrained
End support	Translation in x and y directions is restrained
Loading points	Applied y-displacement
Restraining nodes	Translation in the x-direction is restrained

2.5 Modelling of Fasteners

Shear connectors were modelled using non-linear spring objects provided in Ansys Workbench. Springs are defined as longitudinal, i.e., they connect two nodes in a fixed direction; particleboard on one end of the spring and cold-formed steel joist on the other end. Kyvelou (2017) derived empirical formula (Eq. (3)) based on the data obtained from push-out tests, which describes the shear connectors' load-slip relationship for this specific composite floor. The load-slip response of the shear connectors is illustrated in Fig. 5. Coefficients C_1 and C_2 can be calculated using Eqs. (4)-(5).

$$s = \frac{P}{k_0} + C_1 \left(\frac{P}{P_{10}}\right)^{C_2} \tag{3}$$

$$C_1 = s_{10} - \frac{P_{10}}{k_0} \tag{4}$$

$$C_2 = \frac{\ln\left(s_b - \frac{P_b}{k_0}\right) - \ln(C_1)}{\ln\left(\frac{P_b}{P_{10}}\right)} \tag{5}$$

where,

s is the slip distance,
P is the applied load corresponding to s,
k_0 is slip modulus taken as the slope of the initial part of the push-out curve,
s_{10} is a slip of 10 mm,
P_{10} is the load corresponding to 10 mm slip,
P_b is the bearing capacity of the particleboard, and
s_b is the slip distance corresponding to P_b.

The corresponding values of k_0, s_{10}, P_{10}, P_b, s_b are provided in Table 4. The fasteners' ultimate shear capacity (Pv) is calculated from its dimensions and material properties.

2.6 Modelling of Geometric Imperfections

Geometric imperfection is the deviation of thin-walled sections geometry from their perfect configuration (Dar *et al.* 2019). Accordingly, initial geometric imperfections can generate in cold-formed steel sections as a downside of the cold-forming process. As a result, the ultimate load-carrying capacity of cold-formed steel sections is sensitive to the generated spatial instabilities such as local and distortional buckling.

Thus, Eigenvalue buckling analysis was carried out to account for the initial geometric imperfection in cold-formed steel joists. First, a linear static analysis was carried out on the composite floor, considering the same geometry, boundary conditions, and contacts as the actual non-linear static analysis. The linear analysis was then linked to a downstream eigenvalue finite element analysis from which the lowest buckling mode shape was determined. The lowest buckling mode shape was then assigned to the floor geometry employed in the static non-linear analysis as an initial geometric imperfection by creating a perturbed mesh.

Table 4: Required parameters to establish load-slip response for the shear connectors (Kyvelou *et al.* 2018)

Parameter	Value
k_0 (kN/mm)	1.20
s_{10} (mm)	10
P_{10} (kN)	5.11
P_b (kN)	2.7
s_b (mm)	2.68
P_v (kN)	5.55

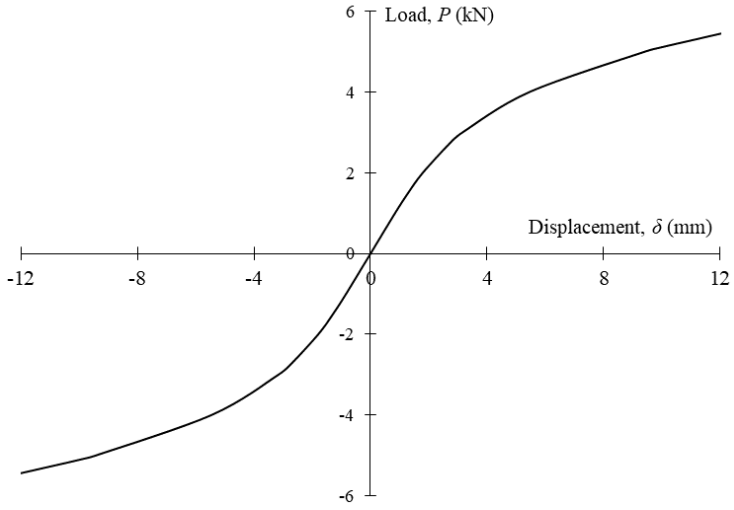

Fig. 5: Adopted load-slip response for the non-linear springs

3. Validation of the Numerical Model

After the creation of the FE model, it was validated against experimental results reported by Kyvelou (2017). The validated model was then utilised to investigate composite floors' dynamic behaviour comprised of cold-formed steel joists and particleboards. Kyvelou (2017) performed four-point bending tests on twelve-floor specimens fabricated from C-shaped cold-formed steel joists and particleboards. Four significant

findings were reported in the experimental study: load-displacement relationship, ultimate moment capacity, flexural rigidity, and normal strain distribution within the cross-section of the floor. Therefore, these four criteria were selected to validate the developed finite element model in this study. Besides, results of floor specimens B15-2 and B30-2 were utilised by Kyvelou *et al.* (2018) to validate their numerical model. Accordingly, the results of floor specimen B30-2 were chosen to validate the finite element model developed in this study because the joist in this floor has a thickness of 3.02 mm, which is similar to cold-formed steel sections available in Australia.

Fig. 7 presents the load-displacement responses of floor B30-2. Load-displacement curves were obtained from three different resources: the finite element model developed in this study, physical tests conducted by Kyvelou (2017), and the numerical analysis reported in (Kyvelou *et al.* 2018). Fig. 6 compares the mode failure observed in physical tests and the mode failure predicted by the FE model in this study. It is evident from Figs. 6-7 that the FE model developed in this study can capture the actual static behaviour observed in the physical tests.

(a) (b)

Fig. 6: Comparison of mode failures; (a) Physical tests and (b) Current FE model.

Moreover, normal strain distribution at mid-span estimated by the finite element model developed in this study is in good agreement with normal strain distribution determined from the physical tests (Kyvelou 2017), as shown in Fig. 8. Furthermore, ratios of ultimate moment capacity and flexural rigidity are 0.98 and 0.99, respectively, compared to the values determined experimentally. As a result, the predicted load-displacement response, failure mode, strain distribution, flexural rigidity, and ultimate moment capacity provide sufficient evidence that the developed numerical model can replicate the actual static behaviour of the investigated composite floors. Finally, since the model is validated, it can be further utilised to investigate the composite floor's vibration behaviour comprised of cold-formed steel joists and particleboard panels. The effects of changing various parameters, such as geometry and degree of shear connection, on such floors' dynamic behaviour will also be studied.

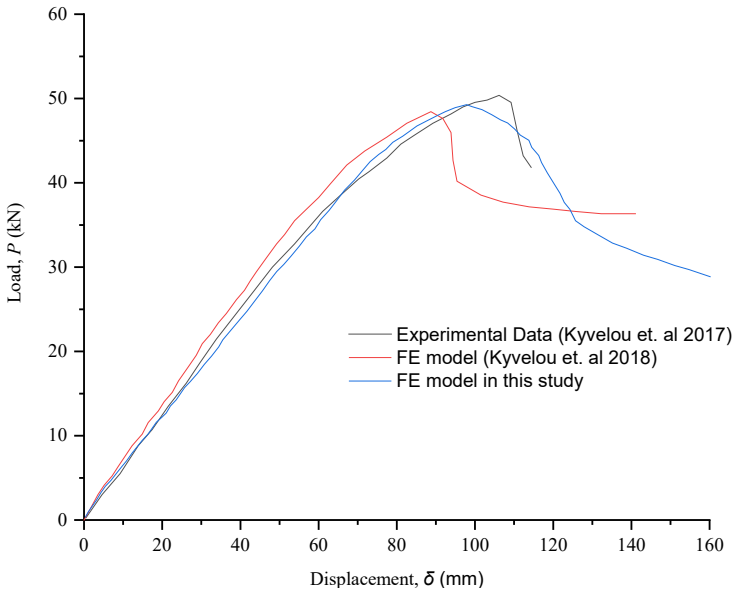

Fig. 7: Comparison of load-displacement curves for B30-2 composite floor.

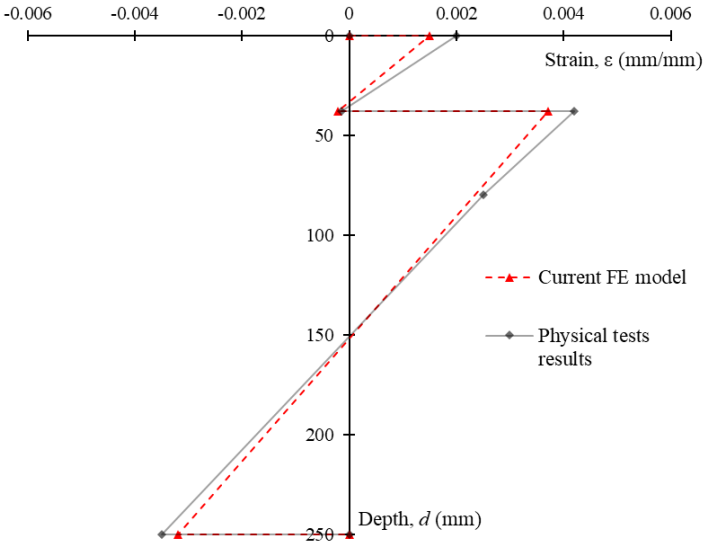

Fig. 8: Normal strain distribution for B30-2 composite floor specimen

4. Vibration of the investigated floors

Once the developed FE model was statically validated, a numerical modal analysis was performed to predict the dynamic properties of the cold-formed steel and particleboard composite flooring system. Then, analytical formulas reported in the literature, which predict the first bending mode's natural frequency, are used to investigate the accuracy of the FE model.

4.1 Modal Analysis Prediction

Once the FE model was validated against the experimental results, a modal analysis was carried out to

extract the natural frequencies and mode shapes required to assess the cold-formed steel and particleboard composite floor's vibration behaviour.

It should be noted that a linear elastic behaviour is assumed for cold-formed steel joists and particleboard panels at service conditions. Also, element types and meshing attributes are similar to those discussed in Section 2.3. Furthermore, a pin connection is considered at each end of the cold-formed steel joists as described in Fig. 4a; however, boundary conditions at loading points were not considered. Additionally, the particleboard panels are considered discontinuous at the joist's ends and can freely rotate. Linear spring elements (COMBIN14) were utilised to model the shear connectors between joists and timber panels. The spring elements' stiffness was taken as the slope of the initial part of the load–slip curve shown in Fig. 5. The gap between two adjacent particleboards was modelled using COMBIN40 spring elements.

Damping was applied to the FE model to account for the damping effects on the investigated composite floors' vibration behaviour. Several researchers, e.g. Feldmann *et al.* (2009); Smith *et al.* (2009), have proposed typical damping values for composite floors. Accordingly, this study adopts a damping ratio of 1.1%, similar to Smith *et al.* (2009), representing bare floors or floors with a minimum amount of furnishings. Although non-structural elements such as furniture and partitions are expected to increase the floor damping significantly, this study investigates the composite floor's vibration performance using a 1.1% damping ratio. Adopting such a relatively low damping ratio is conservative and is expected to reassure designers about the acceptability of the floor vibration performance since it represents the worst-case scenario.

Table 5: Natural frequency of the first ten modes of the investigated floor

Vibration Mode	1	2	3	4	5	6	7	8	9	10
Frequency, f (Hz)	12.509	16.538	21.113	56.895	63.388	73.556	93.639	99.302	102.21	112.52

It should be noted that the FE model developed in this study is part of a broader study that incorporates experimental modal testing of a 1.2 m wide composite beam comprised of cold-formed steel joists and Plywood panels. The study is currently carried out at the University of Technology Sydney (UTS), and the results will be published soon.

Table 5 provides the natural frequencies for the first ten vibration modes. Moreover, mode shapes are shown in Fig. 9. From the results of the modal analysis, the following observations were made:

- The first vibration mode is a torsional mode with a frequency of 12.509 Hz. It is evident from Fig. 9 that the first mode shape is a torsional mode, which indicates that the torsional stiffness of the floor is lower than its bending stiffness. However, torsional modes scarcely dominate the vibration behaviour because, in reality, cold-formed steel and timber composite floor systems are being constructed using continuous timber panels.
- The second vibration mode is the first bending mode of the floor with a natural frequency of 16.538 Hz. According to the Australian standard AS 3623 requirements (Standards Australia 1993), the floor satisfies the specified minimum 8 Hz frequency criterion for high-frequency floors.
- The third vibration mode is the second torsional mode of the composite floor with a natural frequency of 21.113 Hz.
- The fourth mode is the second bending mode. The natural frequency of the second bending mode is 56.895 Hz. According to Rao (2007), the analytical ratio between second and first bending mode frequencies for an ideal simply supported beam is 4, while, in this case, the ratio is 3.44.

- The fifth vibration mode shows a transverse bending mode, indicating that the composite floor's flexural stiffness in the transverse direction is considerably higher than the longitudinal flexural stiffness. The natural frequency of this vibration mode is 63.388 Hz.
- The sixth vibration mode indicates a flexural mode governed mainly by the second bending mode and coupled with a transverse bending mode in the particleboards. The natural frequency for this vibration mode is 73.556 Hz.
- The seventh and eighth vibration modes show the third and fourth bending modes of the composite floor with a natural frequency of 93.639 and 99.302 Hz. The third to the first flexural modes ratio is 5.662; however, for an ideal simply supported beam, the ratio is close to 9 (Rao 2007; Chiniforush *et al.* 2019).
- The ninth and tenth vibration modes are governed mainly by the fourth and fifth flexural modes coupled with transverse bending modes in timber panels.

These results are compared against the minimum fundamental natural frequency criterion set by different design guidelines, e.g. (Standards Australia 1993; European Committee for Standardization 2004; Smith *et al.* 2009; Murray *et al.* 2016) to evaluate the adequacy of the composite floor. The minimum frequency represents a cut off frequency that separates low-frequency flooring systems from high-frequency ones. According to Eurocode 5 and AS 3623, high-frequency floors should have a fundamental natural frequency greater than 8 Hz, whereas the AISC design guideline sets this limit to 9 Hz. The Steel Construction Institute (SCI) (Smith *et al.* 2009) elaborates on the cut off frequency based on the function of the flooring system. Cut off frequencies according to SCI are tabulated in Table (6). According to Bachmann (1987), the walking step frequency ranges from 1.6 to 2.3 Hz. A low-frequency floor's fundamental natural frequency could be excited by one or more of the walking step's harmonic component, which would trigger resonance in the composite flooring system (Smith *et al.* 2009). Floor resonance would considerably discomfort the occupants since human internal organs operate at a frequency range of 4 to 8 Hz (International Organization for Standardization 1989). Thus, designers should avoid low-frequency floors at the conceptual design stage. On the other hand, high-frequency floors provide better vibration performance since their behaviour is controlled by transient response, which corresponds to the heel impacts of occupants.

Based on the preceding discussion, it is evident that the fundamental natural frequency of the composite floor (12.509 Hz) satisfies the high-frequency floors criterion set by different design guidelines, e.g. Standards Australia (1993); European Committee for Standardization (2004); Murray *et al.* (2016). Additionally, static structural results reported by Kyvelou (2017) and the modal analysis results in this study emphasise the potential of cold-formed steel and particleboard composite flooring systems to provide a durable, sustainable, and efficient replacement to the traditional concrete floors in low rise buildings. However, mid-span deflection due to 1 kN point load, velocity and acceleration responses due to human footfall force must be evaluated to further assess the composite floor's adequacy against annoying vibrations.

Table 6: Cut off frequency values of low-frequency floors to high-frequency floors according to SCI (Smith *et al.* 2009).

Floor type	Cut-off frequency, f (Hz)
General floors, Open plan office floor	10
Enclosed floors, e.g. residential floors	8
Staircases	12
Rhythmic activities floors, e.g. dancing floors and gymnasium floors	24

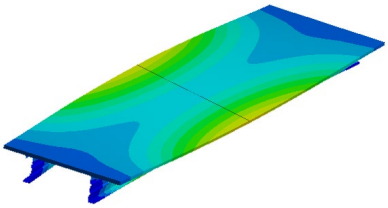

(a) Mode 1: 12.509 Hz

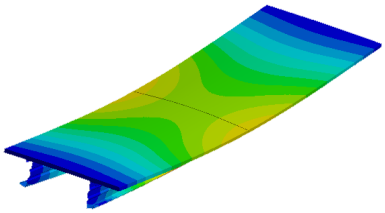

(b) Mode 2: 16.538 Hz

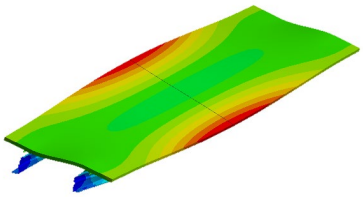

(c) Mode 3: 21.113 Hz

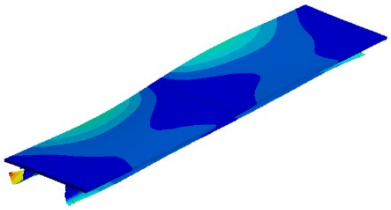

(d) Mode 4: 56.895 Hz

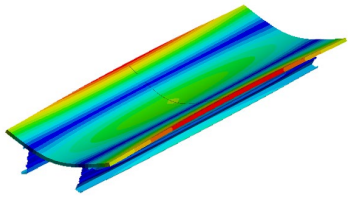

(e) Mode 5: 63.388 Hz

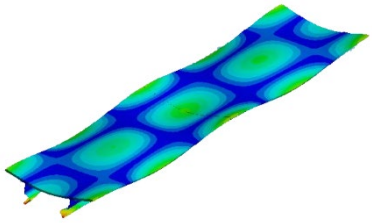

(f) Mode 6: 73.556 Hz

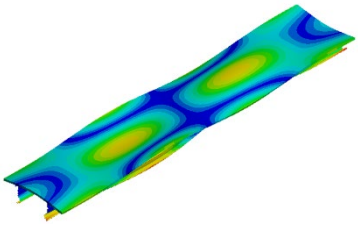

(g) Mode 7: 93.639 Hz

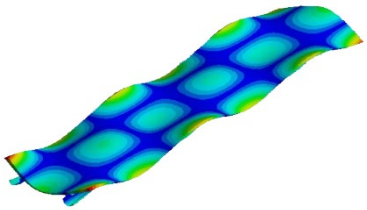

(h) Mode 8: 99.302

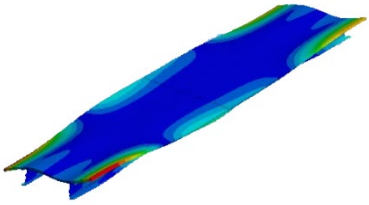

(i) Mode 9: 102.21 Hz

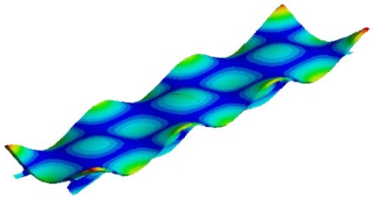

(j) Mode 10: 112.52 Hz

In the following section, analytical formulas to calculate the first flexural frequency of composite floors are discussed.

Fig. 9: The first ten vibration modes of the investigated floor

4.2 Analytical Prediction

The purpose of this section is to examine how accurate the validated FE model can predict the first bending mode's natural frequency. Various analytical relationships (Table 7) have been suggested in the literature to calculate the first bending mode's natural frequency. It is the most critical vibration mode that defines a floor's dynamic behaviour. Predictions from these formulas are compared with the results of the modal analysis.

Table 7: Analytical formulas for predicting the frequency of the first bending mode

Reference	Formula	Description
Wyatt$_1$ (Wyatt 1989)	$f_n = 18/\sqrt{y_0}$	y_0 is the deflection of the floor due to self-weight (w); $\delta_{max} = 5wL^4/384EI$ (mm).
Wyatt$_2$ (Wyatt 1989)	$f_n = C_b\sqrt{EI/mL^4}$	C_b is a constant that defines boundary conditions ($C_b = 1.57$ for pin support)
Murray (Murray *et al.* 2003)	$f_n = (\pi/2)\sqrt{gEI/wL^4}$	EI is the flexural stiffness (Nm^2), w is the weight per unit length (N/m), L is the span length (m).
Eurocode – 5 (European Committee for Standardization 2004)	$f_n = (\pi/2L^2)\sqrt{EI/m}$	EI is the flexural stiffness (Nm^2), m is mass per unit length (kg/m), L is span length (m).
Lei Xu (Xu *et al.* 2018)	$f_n = \pi/2\sqrt{\frac{ab}{m}}\sqrt{\frac{c_1 D_x}{a^4}}$	a is the span length (m), b is the width (m), D_x is the equivalent rigidity in the x-direction (Nm) ($= EI/s$); s is the spacing of fasteners (m). m is the total mass (kg). c_1 is rotational fixity constant ($c_1 = 1$ for pin support)

The primary inputs into the formulas listed in Table 7 are the floor's mass and flexural stiffness (EI). Applied Technology Council (Allen *et al.* 1999) proposed two equations to calculate a composite floor's effective flexural stiffness. Eq. (6) evaluates EI of floors with full composite action, whereas Eq. (7) determines EI for partial composite action floors, as shown in Fig. 9. Furthermore, Kyvelou *et al.* (2017) derived an equation that yields similar results as Eq. (7) to determine the EI value for beams with partial composite action.

$$EI_{\text{eff}} = EI_j + EI_t + \frac{EA_t \times EA_j}{EA_t + EA_j}.z^2 \tag{6}$$

$$EI_{\text{eff}} = EI_j + EI_t + \frac{EA_{ot} \times EA_j}{EA_{ot} + EA_j}.z^2 \tag{7}$$

Where EI_{eff} is the effective flexural stiffness, EI_j and EI_t are the flexural stiffness of the joist and timber, respectively, EA_t and EA_j are the axial stiffness of the timber and joist, respectively, and z is the distance between the neutral axes of the timber and the joist (Fig. 10). EA_{ot} is the modified axial stiffness of the timber given in Eq. (8), where k is the slip modulus, and L is the span length. It is evident from Eq. (8) that the slip modulus is essential to determine the flexural stiffness of a floor with partial composite action.

$$EA_{ot} = \frac{EA_t}{1 + 10\frac{EA_t}{kL^2}} \tag{8}$$

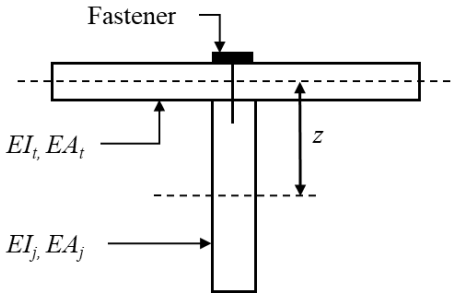

Fig. 10: Illustration of the required properties to calculate EI_{eff} of a composite floor

This study assumes a full composite action between cold-formed steel and timber because unpleasant vibrations have small mid-span vertical deflections; thus, the interface slip is insignificant (Murray *et al.* 2016; Xu *et al.* 2018). Therefore, based on Eq. (6), $EI_{eff} = 3.3778 \times 10^6\ Nm^2$. Besides, the total supported length of the composite floor is 5.8 m, and the mass per unit length of the floor (m) is $22.325\ kg/m$.

The first bending mode frequencies obtained from the analytical formulas and modal analysis are provided in Table 8. Comparing results obtained from the FE model and analytical formulas, the FE model can predict the first bending mode's natural frequency with sufficient accuracy considering the uncertainty in boundary conditions, material properties, discontinuities, and degree of composite action. The validated numerical model predicts the composite floor's natural frequency with a maximum error of 4.05% and a mean error of 2.90%.

Table 8: Comparison between analytical and FE model predictions of first bending mode's frequency

Reference	Frequency (Hz)	Error (%)
FE model	16.538	–
Wyatt$_1$	17.208	4.05
Wyatt$_2$	16.964	2.58
Murray	16.972	2.62
Eurocode – 5	16.972	2.62
Lei Xu	16.973	2.63
		Mean Error = 2.90 %

4.3 Influence of various floor details on the vibration behaviour

This section investigates the effect of changing different parameters on the vibration behaviour of the composite floor. The discussion regarding the influence of joist thickness, shear connection spacing, span length, and various types of timber panels on the composite floor's vibration behaviour is based on the modal analysis results, which utilises the validated FE model. Those parameters' effects are compared based on the natural frequency values of the composite floor's first four vibration modes. In all comparisons, only the parameter being investigated was modified while all other parameters were kept constant. The considered parameters and their values are listed in Table 9. The default parameter values are identical to those discussed in Section 2.1. The influence of different parameters on the composite floor's vibration behaviour is illustrated in Fig. 11. It is observed that, in most cases, the fundamental natural frequency of the cold-formed steel and timber composite floors is higher than 8 Hz except for floors with span length more than 8.0 m and floors with joist thickness of less than 1.2 mm.

Table 9: List of influential parameters on the dynamic performance of the composite flooring system

	Parameter	Value
1	Joist thickness, *t* (mm)	(a) 1.0, (b) 1.2, (c) 1.5, (d) 1.9, (e) 2.4
2	Timber material properties	(a) Oriented strand board (OSB) (b) Laminated veneer lumber (LVL) (c) Cross-laminated timber (CLT) (d) Laminated Moso bamboo
3	Spacing of shear connectors, *S* (mm)	(a) 600, (b) 300, (c) 200, (d) 150
4	Span length, *L* (m)	(a) 4.0, (b) 6.0, (c) 8.0, (d) 10.0

4.3.1 *Influence of joist thickness*

Various joist thickness values were studied to assess their influence on the vibration behaviour of the composite floor. The investigated thicknesses are based on the joist thicknesses available in the Australian market. According to Fig. 11(a), floors with thicker cold-formed steel joists have higher natural frequencies. For instance, floors supported by 1.0 mm thick joists have a fundamental natural frequency of 5.576 Hz compared to 12.509 Hz for floors with 3.02 mm thick joists with a 224% increase in the fundamental natural frequency. As a result, it has become apparent that the joist's thickness significantly impacts the floor's natural frequencies. This increase is attributed to the floor's flexural stiffness provided by the cold-formed steel joist.

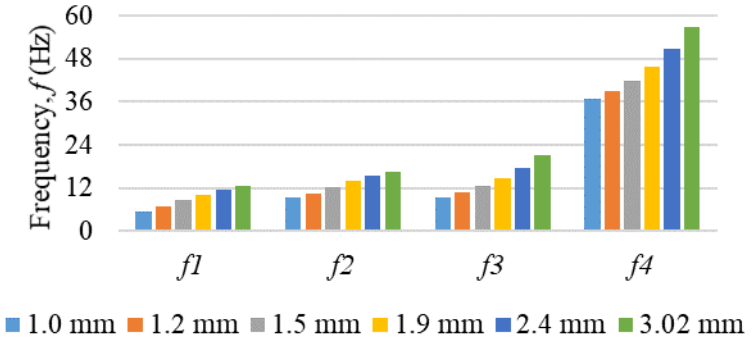

(a)

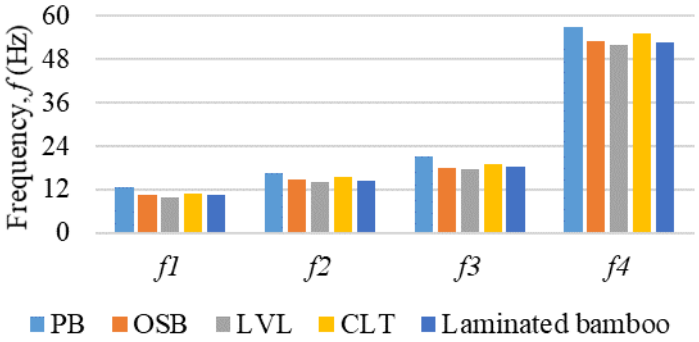

(b)

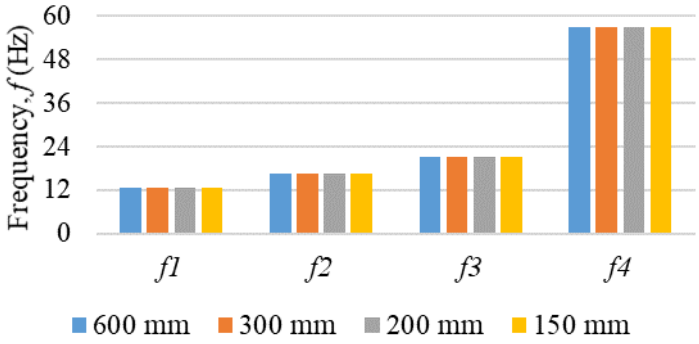

(c)

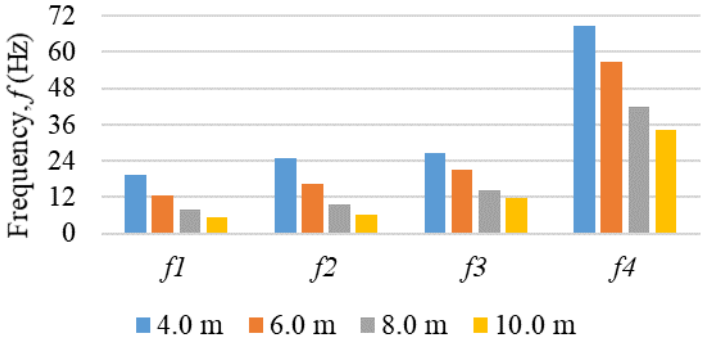

(d)

Fig. 11: Comparison of the first four vibration modes frequencies with different (a) Joist thickness, (b) Engineered wood products, (c) Spacing of shear connectors, (d) Span length

4.3.2 *Influence of timber material properties*

Commercially available engineered wood products, such as Oriented Strand Boards (OSB), provide a sustainable solution to replace particleboard in the cold-formed steel-particleboard composite flooring systems. Therefore, the validated FE model was used to study the composite floor's vibrational behaviour, replacing particleboards with several engineered wood products. The orthotropic elastic properties of the considered engineered wood products are provided in Table 10. These properties are based on data reported by several researchers, e.g. (Bai *et al.* 1999; Janowiak *et al.* 2001; Chen and He 2017).

Table 10: Mechanical properties of different timber types adopted in the parametric study

Timber ID	Young's Modulus (MPa)			Shear Modulus (MPa)			Poisson's ratio		
	E_1	E_2	E_3	G_{12}	G_{13}	G_{23}	υ_{12}	υ_{13}	υ_{23}
Particleboard (Kyvelou *et al.* 2017)	2,300	2,300	2,300	958	958	958	0.20	0.20	0.20
Southern pine OSB (Chen and He 2017)	4,000	2,400	690	690	207	170	0.15	0.30	0.30
Southern pine LVL (Janowiak *et al.* 2001)	16,100	1,600	570	754	403	120	0.52	0.35	0.40
CLT (Chiniforush *et al.* 2019)	13,200	700	700	800	800	140	0.48	0.48	0.22
Laminated Moso Bamboo (Bai *et al.* 1999)	10,350	500	690	830	900	290	0.39	0.34	0.31

As described in Section 4.1, linear modal analyses were carried out using engineered wood mechanical properties listed in Table 9 and identical floor details of the validated FE model. The predicted numerical fundamental frequencies of the first four vibration modes for various composite floors with different engineered wood products are tabulated in Table 11 and illustrated in Fig. 11(b). Comparing the results in Table 11 shows that floors with particleboards yield the highest fundamental natural frequency. Replacing particleboards with OSB, Laminated Veneer Lumber (LVL), Cross Laminated Timber (CLT), and laminated bamboo reduced the fundamental natural frequency by 19.5%, 27.2%, 15.6%, and 19.8%, respectively. Therefore, it is recommended that designers be careful in replacing isotropic timber material with an orthotropic engineered wood product. It is also advisable that builders pay careful attention to the strong axis orientation of stratified engineered wood products (such as CLT, LVL, and Plywood) since this would affect the floor's fundamental natural frequency, as concluded by several studies (Chiniforush *et al.* 2019). The fundamental natural frequency for those floors is higher when the joist and timber strong axes are parallel.

The observed reduction in the natural frequencies was probably because of the low transverse Young's moduli (E_2 and E_3) and low out-of-plane shear moduli (G_{13} and G_{23}) of the engineered wood products compared to transverse Young's modulus of the particleboard (2300 MPa) and its out-of-plane shear modulus (958 MPa). Based on that, OSB, LVL, CLT, and laminated bamboo orthotropic elastic properties have a considerable influence on the dynamic performance of the cold-formed steel-timber composite flooring systems. However, the fundamental natural frequency is more than 8 Hz for all composite floors utilising engineered wood products. Therefore, PB, OSB, LVL, CLT, and laminated bamboo can be considered in designing composite floors comprised of cold-formed steel joists and timber panels.

Table 11: Natural frequencies of the first four vibration modes for different engineered wood products

Engineered wood product	Natural Frequency (Hz)			
	f_1	f_2	f_3	f_4
Particleboard	12.509	16.538	21.113	56.895
Southern pine OSB	10.472	14.633	17.945	53.04
Southern pine LVL	9.834	14.03	17.39	51.97
Cross Laminated Timber (CLT)	10.823	15.393	18.79	55.07
Laminated Moso bamboo	10.44	14.37	18.375	52.68

4.3.3 *Influence of shear connectors spacing*

In the construction of composite floors, the cold-formed steel joists and particleboards panels were mechanically joined together using self-tapping screws. Various screw spacing is utilised in construction practice; typical screw spacing is 150 mm and 300 mm (Xu 2011). Closer screw spacing results in higher stiffness of the composite flooring system and less mid-span deflection (Mirambell *et al.* 2021), which would affect their vibration performance acceptability. Therefore, this study investigates the influence of different screw spacing on the dynamic behaviour of such floors.

Modal analysis results illustrated in Fig. 11(c) show that increasing the number of screws has a minor effect on the natural frequencies of the first four vibration modes. Despite reducing the screw spacing from 300 mm to 150 mm, a slight increase (less than 5%) in the natural frequencies was observed. The negligible effect of the screw spacing is attributed to the fact that annoying vibrations have small mid-span vertical deflections; hence, the interface slip between cold-formed steel joist and particleboards panels is insignificant and full composite action is assumed (Murray *et al.* 2016; Xu *et al.* 2018).

Alternatively, spacing of shear connectors has had a more significant effect on the mid-span deflection of the floor as illustrated in Table 12. It is observed that increasing screw spacing results in higher mid-span deflection, which would result in unsatisfactory vibration performance of the floor system since different standards adopt mid-span deflection criteria to assess floor vibrations. For instance, according to Swedish standards requirements (Zhang *et al.* 2013), the mid-span deflection due to 1 kN static point load is limited to 1.50 mm. Consequently, composite floors with shear connector spacing of 200, 300, and 600 mm have unacceptable vibration behaviour. In contrast, AS 3623 limits the deflection due to a 1 kN static point load applied anywhere on the floor to 2 mm. Results provided in Table 12 show that the mid-span deflection criterion specified in AS 3623 is satisfied for all cases of shear connector spacing. However, Krause (1997) argued that the Australian criteria are excessively tolerant in assessing floor vibrations. Therefore, it is recommended that AS 3623 be revised and updated to prevent negative comments from arising due to annoying vibrations.

Table 12: Mid-span deflection due to 1 kN concentrated load for different spacing of shear connectors

Shear connectors Spacing, S (mm)	Mid-span deflection, δ (mm)
150	1.47
200	1.51
300	1.56
600	1.69

4.3.4 *Influence of span length*

The natural frequencies of the first four vibration modes are listed in Table 13 and illustrated in Fig. 11(d) for different span lengths. Comparing the results in Fig. 11(d) indicates that span length significantly influences the natural frequencies of the composite floor system. A 4 m long composite floor has a fundamental natural frequency of 19.544 Hz. In contrast, it is 7.952 Hz for a composite floor with an 8 m span length, i.e. reducing the span length from 8.0 m to 4.0 m increased the fundamental natural frequency by 2.458 times. Moreover, composite flooring systems with a span length of more than 8.0 m are more vulnerable to annoying vibrations since their fundamental natural frequencies are less than the 8 Hz limit (e.g. Standards Australia 1993; European Committee for Standardization 2004; Murray *et al.* 2016). Eurocode 5 states that an elaborated method is required to assess the floor adequacy against uncomfortable floor vibrations if its fundamental natural frequency falls below 8 Hz. AS 3623, on the other hand, does not provide any guidance in such a case.

Considering the natural frequencies for different span lengths (Table 13), it is evident that the span length considerably affects the floor system's stiffness, especially the flexural stiffness, which explains its significant influence on the natural frequencies of the composite flooring system. The equations listed in Table 6 also demonstrate the inverse relationship between the fundamental natural frequency and the span length.

Table 13: Natural frequencies of the first four vibration modes for different span lengths

Span length, L (m)	Natural frequency, f_n (Hz)			
	f_1	f_2	f_3	f_4
4.0	19.544	24.987	26.748	68.598
6.0	12.509	16.538	21.113	56.895
8.0	7.952	9.70	14.332	41.736
10.0	5.50	6.24	11.735	34.412

5. Conclusion

Cold-formed steel and timber composite flooring systems are susceptible to annoying vibrations at service loading conditions due to their lightness and relatively low damping. Therefore, it is essential to assess their dynamic behaviour thoroughly during the conceptual design stage.

This study investigates the vibration performance of a composite floor system comprising cold-formed steel joists and particleboards panels. It further examines the influence of various floor details on the dynamic behaviour of the composite floor system. First, a FE model was developed and validated against available experimental results. Modal analysis was then carried out to explore the vibration characteristics of the cold-formed steel and particleboard flooring system, including natural frequencies, mode shapes, and modal mass. The first bending mode frequency predicted by the FE model was verified using analytical formulas reported in the literature. The FE model accurately predicted the first bending mode frequency with an average error of 2.9%. Based on the numerical investigation outcomes, it is apparent that the predicted first vibration mode frequency of the studied composite floor meets the minimum frequency criteria set by different design guidelines such as Australian standard AS 3623, AISC design guide 11, and Eurocode 5.

The validated FE model explored the effects of joist thickness, timber material properties, shear connectors spacing, and span length. The thickness of the cold-formed steel joist and the span length were the two most influential parameters on the composite floor vibration performance due to their considerable contribution to flexural stiffness. The spacing of the shear connectors had a minimal effect on the floor's natural frequencies. However, fasteners' spacing substantially affects the composite floor's maximum deflection under the action of 1 kN concentrated load at mid-span. Wider spacing will produce higher mid-span deflection, which would result in unsatisfactory vibration behaviour if the deflection limit is exceeded. Furthermore, the natural frequencies of the composite floor system were sensitive to timber orthotropic elastic properties; thus, it is recommended that designers and builders pay particular attention to the timber's strong axis orientation.

Modal analysis results show that cold-formed steel and particleboard composite flooring systems meet serviceability limit state requirements, particularly the floor vibration criteria. However, further research is recommended to investigate the floor's maximum velocity and acceleration responses to ensure its vibration performance adequacy. Accordingly, such study with more detailed investigation is currently underway at the University of Technology Sydney. Results in this study are based on the numerical investigation of the composite floor vibration behaviour. The findings of this study provide insight into the dynamic behaviour of lightweight composite floors and endorse the cold-formed steel and timber composite floor as a sustainable and cost effective floor solution. Additionally, findings can be utilised to develop analytical formulae that can be adopted by design standards. These formulae will help designers to determine the vibration response of lightweight composite floors at the design stage and avoid expensive repairs in the future.

References

Afshan, S., Rossi, B. and Gardner, L. (2013), "Strength enhancements in cold-formed structural sections — Part I: Material testing", *Journal of Constructional Steel Research*. **83**, 177-188. https://doi.org/10.1016/j.jcsr.2012.12.008

Allen, D.E., Onysko, D.M. and Murray, T.M. (1999), Minimising floor vibration, Applied Technology Council, Redwood City, CA, USA.

Ataei, A., Bradford, M.A. and Valipour, H.R. (2016), "Finite element analysis of HSS semi-rigid composite joints with precast concrete slabs and demountable bolted shear connectors", *Finite Elements in Analysis and Design*. **122**, 16-38. https://doi.org/10.1016/j.finel.2016.08.003

Bachmann, H. (1987), *Vibrations in structures, induced by man and machines*, International Association for Bridge and Structural Engineering, Zurich, Switzerland.

Bachmann, H., Ammann, W.J., Deischl, F., Eisenmann, J., Floegl, I., Hirsch, G.H., Klein, G.K., Lande, G.J., Mahrenholtz, O., Natke, H.G., Nussbaumer, H., Pretlove, A.J., Rainer, J.H., Saemann, E.-U. and Steinbeisser, L. (1995), *Vibration Problems in Structures*, Birkhäuser Basel, Basel.

Bai, X., Lee, A.W.C., Thompson, L.L. and Rosowsky, D.V. (1999), "Finite element analysis of Moso bamboo-reinforced southern pine OSB composite beams", *Wood and Fiber Science*. **31**(4), 403-415.

Cao, L., Li, J., Zheng, X. and Chen, Y.F. (2020), "Vibration behavior of large span composite steel bar truss-reinforced concrete floor due to human activity", *Steel and Composite Structures*. **37**(4), 391-404. https://doi.org//10.12989/scs.2020.37.4.391

Cao, L., Tan, Y. and Li, J. (2021), "Experimental studies on vibration serviceability of composite steel-bar truss slab with steel girder under human activities", *Steel and Composite Structures*. **40**(5), 663-678.

Casagrande, D., Giongo, I., Pederzolli, F., Franciosi, A. and Piazza, M. (2018), "Analytical, numerical and experimental assessment of vibration performance in timber floors", *Engineering Structures*. **168**(July 2017), 748-758. https://doi.org/10.1016/j.engstruct.2018.05.020

Chen, G. and He, B. (2017), "Stress-strain constitutive relation of OSB under axial loading: An experimental investigation", *BioResources*. **12**(3), 6142-6156. https://doi.org/10.15376/biores.12.3.6142-6156

Chiniforush, A., Makki Alamdari, M., Dackermann, U., Valipour, H.R. and Akbarnezhad, A. (2019), "Vibration behaviour of steel-timber composite floors, part (1): Experimental & numerical investigation", *Journal of Constructional Steel Research*. **161**, 244-257. https://doi.org/10.1016/j.jcsr.2019.07.007

Dar, M.A., Subramanian, N., Dar, A.R., Majid, M., Haseeb, M. and Tahoor, M. (2019), "Structural efficiency of various strengthening schemes for cold-formed steel beams: Effect of global imperfections", *Steel and Composite Structures*. **30**(4), 393-403. https://doi.org/10.12989/scs.2019.30.4.393

Dodoo, A., Gustavsson, L. and Sathre, R. (2014), "Lifecycle carbon implications of conventional and low-energy multi-storey timber building systems", *Energy and Buildings*. **82**, 194-210. https://doi.org/10.1016/j.enbuild.2014.06.034

Ebrahimpour, A. and Sack, RL (1992), "Design Live Loads for Coherent Crowd Harmonic Movements", *Journal of Structural Engineering*. **118**(4), 1121-1136. https://doi.org/10.1061/(ASCE)0733-9445(1992)118:4(1121)

EN 1995-1-1 (2004), Eurocode 5: Design of timber structures-Part 1-1: General-Common rules and rules for buildings, European Committee for Standardization; Brussels, Belgium.

Far, H. (2020), "Flexural Behavior of Cold-Formed Steel-Timber Composite Flooring Systems", *Journal of Structural Engineering (United States)*. **146**(5), 1-6. https://doi.org/10.1061/(ASCE)ST.1943-541X.0002600

Far, H., Saleh, A., and Firouzianhaji, A. (2017), "A simplified method to determine shear stiffness of thin walled cold formed steel storage rack frames", *Journal of Constructional Steel Research*, **138**, 799-805. https://doi.org/10.1016/j.jcsr.2017.09.012

Saleh, A., Far, H., and Mok, L. (2018), "Effects of different support conditions on experimental bending strength of thin walled cold formed steel storage upright frames," *Journal of constructional steel research*, **150**, 1-6.https://doi.org/10.1016/j.jcsr.2018.07.031

Feldmann, M., Heinemeyer, C., Butz, C., Caetano, E., Cunha, Á., Galanti, F. and Goldack, A. (2009), "Design

of floor structures for human induced vibrations, JRC-ECCS Joint Report", JRC 55118; JRC-Scientific and Technical Report.

Gardner, L. and Ashraf, M. (2006), "Structural design for non-linear metallic materials", *Engineering Structures*. **28**(6), 926-934. https://doi.org/10.1016/j.engstruct.2005.11.001

Gerilla, G.P., Teknomo, K. and Hokao, K. (2007), "An environmental assessment of wood and steel reinforced concrete housing construction", *Building and Environment*. **42**(7), 2778-2784. https://doi.org/10.1016/j.buildenv.2006.07.021

Guan, Y., Zhou, X., Yao, X. and Shi, Y. (2019), "Vibration of cold-formed steel floors with a steel form deck and gypsum-based self-leveling underlayment", *Advances in Structural Engineering*. **22**(13), 2741-2754. https://doi.org/10.1177/1369433219849836

Hassanieh, A., Chiniforush, A.A., Valipour, H.R. and Bradford, M.A. (2019), "Vibration behaviour of steel-timber composite floors, part (2): Evaluation of human-induced vibrations", *Journal of Constructional Steel Research*. **158**, 156-170. https://doi.org/10.1016/j.jcsr.2019.03.026

Hsu, C.-T.T., Punurai, S., Punurai, W. and Majdi, Y. (2014), "New composite beams having cold-formed steel joists and concrete slab", *Engineering Structures*. **71**, 187-200. https://doi.org/10.1016/j.engstruct.2014.04.011

ISO 2631-2 (1989), Evaluation of human exposure to whole-body vibration — Part 2: Continuous and shock-induced vibrations in buildings (1 to 80 Hz), International Organization for Standardization; Geneva, Switzerland.

ISO 10137 (2007), Bases for design of structures-Serviceability of buildings and walkways against vibrations, International Organization for Standardization; Geneva, Switzerland.

Janowiak, J.J., Hindman, D.P. and Manbeck, H.B. (2001), "Orthotropic behavior of lumber composite materials", *Wood and Fiber Science*. **33**(4), 580-594.

Karki, D. and Far, H. (2021), "State of the art on composite cold-formed steel flooring systems", *Steel Construction*. **14**, 1-11. https://doi.org/10.1002/stco.202000026

Karren, K.W. (1967), Effects of cold-forming on light-gage steel members,

Krause, M. (1997), "Floor Vibration Design Criterion For Cold-Formed C-Shaped Supported Residential Floor Systems", Virginia Polytechnic Institute and State University, VA, United States.

Kyvelou, P. (2017), "Structural behaviour of composite cold-formed steel systems", Ph.D. Dissertation; Imperial College London, London, UK.

Kyvelou, P., Gardner, L. and Nethercot, D.A. (2015), "Composite Action between Cold-Formed Steel Beams and Wood-Based Floorboards", *International Journal of Structural Stability and Dynamics*. **15**(8), 1-17. https://doi.org/10.1142/S0219455415400295

Kyvelou, P., Gardner, L. and Nethercot, D.A. (2017), "Design of Composite Cold-Formed Steel Flooring Systems", *Structures*. **12**, 242-252. https://doi.org/10.1016/j.istruc.2017.09.006

Kyvelou, P., Gardner, L. and Nethercot, D.A. (2017), "Testing and Analysis of Composite Cold-Formed Steel and Wood-Based Flooring Systems", *Journal of Structural Engineering (United States)*. **143**(11), 1-16. https://doi.org/10.1061/(ASCE)ST.1943-541X.0001885

Kyvelou, P., Gardner, L. and Nethercot, D.A. (2018), "Finite element modelling of composite cold-formed steel flooring systems", *Engineering Structures*. **158**(May 2017), 28-42. https://doi.org/10.1016/j.engstruct.2017.12.024

Kyvelou, P., Reynolds, T., Beckett, C., Wong, P.W. and Huang, Y. (2018). "Composite panels of cold-formed steel and timber for high- density construction", *2018 World Conference on Timber Engineering, WCTE 2018*, Seoul, Republic of Korea, August.

Liu, J., Cao, L. and Chen, Y.F. (2019), "Vibration performance of composite steel-bar truss slab with steel girder", *Steel and Composite Structures*. **30**(6), 577-589. https://doi.org/10.12989/scs.2019.30.6.577

Loss, C., Piazza, M. and Zandonini, R. (2016), "Connections for steel–timber hybrid prefabricated buildings. Part II: Innovative modular structures", *Construction and Building Materials*. **122**, 796-808. https://doi.org/10.1016/j.conbuildmat.2015.12.001

Middleton, C.J. and Brownjohn, J.M.W. (2010), "Response of high frequency floors: A literature review", *Engineering Structures*. **32**(2), 337-352. https://doi.org/10.1016/j.engstruct.2009.11.003

Mirambell, E., Bonilla, J., Bezerra, LM and Clero, B. (2021), "Numerical study on the deflections of steel-concrete composite beams with partial interaction", *Steel and Composite Structures*. **38**(1), 67-78. https://doi.org/10.12989/scs.2021.38.1.067

Mohammed, A.S., Pavic, A. and Racic, V. (2018), "Improved model for human induced vibrations of high-frequency floors", *Engineering Structures*. **168**(May), 950-966. https://doi.org/10.1016/j.engstruct.2018.04.093

Mulas, M.G., Lai, E. and Lastrico, G. (2018), "Coupled analysis of footbridge-pedestrian dynamic interaction", *Engineering Structures*. **176**(September), 127-142. https://doi.org/10.1016/j.engstruct.2018.08.055

Murray, T.M., Allen, D.E. and Ungar, E.E. (2003), AISC Design guide 11 2nd ed., *Floor vibrations due to human activities*, American Institute of Steel Construction, United States.

Murray, T.M., Allen, D.E., Ungar, E.E. and Davis, D.B. (2016), AISC Design Guide 11, *Vibrations of Steel-Framed Structural Systems Due to Human Activity*, American Institute of Steel Construction, United States of America.

Natário, P., Silvestre, N. and Camotim, D. (2014), "Computational modelling of flange crushing in cold-formed steel sections", *Thin-Walled Structures*. **84**, 393-405. https://doi.org/10.1016/j.tws.2014.07.006

Navaratnam, S., Widdowfield Small, D., Gatheeshgar, P., Poologanathan, K., Thamboo, J., Higgins, C. and Mendis, P. (2021), "Development of cross laminated timber-cold-formed steel composite beam for floor system to sustainable modular building construction", *Structures*. **32**, 681-690. https://doi.org/https://doi.org/10.1016/j.istruc.2021.03.051

Parnell, R., Davis, B.W. and Xu, L. (2010), "Vibration Performance of Lightweight Cold-Formed Steel Floors", *Journal of Structural Engineering*. **136**(6), 645-653. https://doi.org/10.1061/(ASCE)ST.1943-541X.0000168

Pernica, G. (1990), "Dynamic load factors for pedestrian movements and rhythmic exercises", *Canadian Acoustics*. **18**(2), 3-18.

Racic, V., Pavic, A. and Brownjohn, J.M.W. (2009), "Experimental identification and analytical modelling of human walking forces: Literature review", *Journal of Sound and Vibration*. **326**(1-2), 1-49. https://doi.org/10.1016/j.jsv.2009.04.020

Rack, W. and Lange, J. (2010), Human induced vibrations of lightweight floor systems supported by cold-formed steel joists, *Advances and Trends in Structural Engineering, Mechanics and Computing*, Cape Town, South Africa.

Rainer, J.H. and Pernica, G. (1986), "Vertical dynamic forces from footsteps", *Canadian Acoustics*. **14**(2), 12-21.

Ramberg, W. and Osgood, W.R. (1943), "Desription of stress-strain curves by three parameters", National Advisory Committee for Aeronautics.

Rao, S.S. (2007), *Vibration of Continuous Systems*, John Wiley & Sons Inc., Hoboken, New Jersey, United States.

Smith, A.L., Hicks, S.J. and Devine, P.J. (2009), Design of floors for vibration: A new approach, Steel Construction Institute Ascot, Berkshire, UK

AS 3623 (1993), Domestic Metal Framing (Reconfirmed in 2018), Standards Australia; NSW, Australia.

Tangorra, F.M., Xu, L. and Xie, W.C. (2002). "Vibration characteristics of lightweight floors using cold-formed steel joist", *16th International Specialty Conference on Cold-Formed Steel Structures*, Orlando, Florida, October.

Thirunavukkarasu, K., Kanthasamy, E., Gatheeshgar, P., Poologanathan, K., Rajanayagam, H., Suntharalingam, T. and Dissanayake, M. (2021), "Sustainable Performance of a Modular Building System Made of Built-Up Cold-Formed Steel Beams", *Buildings*. **11**(10), 460.

Vasdravellis, G., Uy, B., Tan, E.L. and Kirkland, B. (2015), "Behaviour and design of composite beams subjected to sagging bending and axial compression", *Journal of Constructional Steel Research*. **110**, 29-39. https://doi.org/10.1016/j.jcsr.2015.03.010

Wyatt, T.A. (1989), *Design guide on the vibration of floors*, Steel Construction Institute, Ascot, Berkshire, UK

Xu, L. (2011), "Floor vibration performance of lightweight cold-formed steel framing", *Advances in Structural Engineering*. **14**(4), 659-672.

Xu, L. and Tangorra, F.M. (2007), "Experimental investigation of lightweight residential floors supported by cold-formed steel C-shape joists", *Journal of Constructional Steel Research*. **63**(3), 422-435. https://doi.org/10.1016/j.jcsr.2006.05.010

Xu, L., Zhang, S. and Yu, C. (2018), "Determination of equivalent rigidities of cold-formed steel floor systems for vibration analysis, Part II: evaluation of the fundamental frequency", *Thin-Walled Structures*. **132**, 1-15. https://doi.org/10.1016/j.tws.2018.08.002

Zhang, B., Rasmussen, B., Jorissen, A. and Harte, A. (2013), "Comparison of vibrational comfort assessment criteria for design of timber floors among the European countries", *Engineering Structures*. **52**, 592-607. https://doi.org/10.1016/j.engstruct.2013.03.028

Zhang, S., Xu, L. and Qin, J. (2017), "Vibration of lightweight steel floor systems with occupants: Modelling, formulation and dynamic properties", *Engineering Structures*. **147**, 652-665. https://doi.org/10.1016/j.engstruct.2017.06.008

Zhou, X., Shi, Y., Xu, L., Yao, X. and Wang, W. (2018), "A simplified method to evaluate the flexural capacity of lightweight cold-formed steel floor system with oriented strand board subfloor", *Thin-Walled Structures*. **134**, 40-51. https://doi.org/10.1016/j.tws.2018.09.006

Zhu, L., Yang, Y., Wang, Z. and Song, M. (2016), "Stability Analyses of the Upper Chord Tubes of Light Gauge Steel–Oriented Strand Board Composite Truss Girders", *International Journal of Structural Stability and Dynamics*. **16**(01), 1640012-1640012. https://doi.org/10.1142/S0219455416400125